$[MeNC_5H_5]_2[TCNE]_2$ (TCNE = tetracyanoethylene). Single crystal X-ray and neutron diffraction characterization of an exceptionally long 2.8 Å C–C bond†

Paula M. B. Piccoli,[a] Arthur J. Schultz,[a] Hazel A. Sparkes,[b] Judith A. K. Howard,[b] Atta M. Arif,[c] Louise N. Dawe[c] and Joel S. Miller*[c]

Received 8th October 2008, Accepted 25th November 2008
First published as an Advance Article on the web 8th January 2009
DOI: 10.1039/b816817b

The reaction of *N*-methylpyridinium iodide, $Mepy^+I^-$, and tetracyanoethylene (TCNE) forms $[Mepy]_2[TCNE]_2$, which possesses $[TCNE]_2^{2-}$ with an intradimer C–C bond distance of 2.806(1) Å at 50 K from X-ray diffraction, and 2.801(4) Å at 50 K from neutron diffraction. In the IR it exhibits $\nu_{C\equiv N}$ absorptions at 2191, 2174, 2169, 2163 and a ν_{CC} absorption at 1366 cm^{-1}, with UV/Vis absorption bands at 26,880 and 18,520 cm^{-1}. Analysis of the cation-hydrogen to $[TCNE]_2^{2-}$ interactions do not provide evidence that the cation stabilizes formation of the $[TCNE]_2^{2-}$ dimer, which is stabilized by the intradimer $2e^-$-4 center C–C bonding interaction.

Introduction

Interest in organic compounds exhibiting unusually long C–C bonds has been the subject of several recent studies.[1–3] While the longest sp^3-sp^3 CC single bond reported to date is ~2.0 Å,[4] π-$[TCNE]_2^{2-}$ (TCNE = tetracyanoethylene) dimers form long, two-electron C–C bonds involving four carbon atoms, $2e^-$/4c. These long C–C bonds range from 2.83 to 3.09 Å,[5–7] and are independent of the cations that span from electrostatically bonded Tl^+[8] to large bulky non-coordinating cations such as $[TDAE]^{2+}$ [TDAE = $(Me_2N)_2CC(NMe_2)_2$].[9]

The π-$[TCNE]_2^{2-}$ dimer is electronically best described as the b_{2g} SOMOs on the two $[TCNE]^{\bullet-}$ fragments interacting to form dimer b_{2u} HOMO bonding and b_{1g} LUMO antibonding orbitals (Fig. 1).[3–7] Hence, the $[TCNE]_2^{2-}$ HOMO has the $2e^-$ equally distributed over the four central C atoms.

As part of our ongoing studies into multicenter C–C bonding, we have sought new examples, and in particular ones that form large crystals to enable their structure determination *via* single crystal neutron diffraction, importantly providing more accurate bond distances and angles to fully characterize the multicentre nature of the C–C bonding. Herein, we report the X-ray and neutron diffraction structure determination of methyl pyridinium tetracyanoethylenide, $[Mepy]_2[TCNE]_2$ (py = NC_5H_5), which to date has the shortest C–C bond reported for this family of compounds.

[a]*Intense Pulsed Neutron Source, Argonne National Laboratory, Argonne, IL, 60439-4814, USA*
[b]*University of Durham, Department of Chemistry, South Road, Durham, UK DH1 3LE*
[c]*Department of Chemistry, University of Utah, 315 S. 1400 E. RM 2124, Salt Lake City, UT, 84112-0850, USA. E-mail: jsmiller@chem.utah.edu*
† Electronic supplementary information (ESI) available: Intra $[TCNE]_2^{2-}$ bond distances, torsion angles, and intermolecular contacts for $[Mepy]_2[TCNE]_2$. CCDC reference numbers 256746, 214705, and 700951. For ESI and crystallographic data in CIF or other electronic format see DOI: 10.1039/b816817b

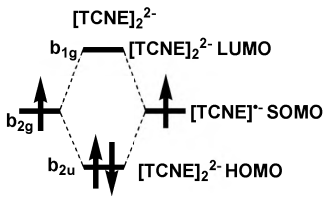

Fig. 1 MO diagram arising from the overlap of two b_{2g} SOMOs on each $[TCNE]^{\bullet-}$ forming the $[TCNE]_2^{2-}$ b_{2u} HOMO and b_{1g} LUMO.

Experimental

Synthesis

Due to the extreme air/water sensitivity of the $[TCNE]^{\bullet-}$, all manipulations and reactions were performed in a Vacuum Atmospheres DriLab glove box (<1-ppm O_2 and <1-ppm H_2O). Et_2O was distilled from sodium/benzophenone and MeCN was purified by passing it through two alumina columns under nitrogen. Pyridine and iodomethane were used as received, and TCNE was sublimed prior to use.

A solution of iodomethane (MeI) (2.28 g, 16.1 mmol) in 5 mL of diethyl ether was slowly added to a stirred solution of pyridine (py) (1.96 g, 24.7 mmol) in 5 mL of diethyl ether. The reaction solution was stirred for 1 h while cooled with an ice/water bath. White, powdery [Mepy]I was collected by filtration and was washed three times with 3 mL of diethyl ether (28.2% yield).

The synthesis of $[Mepy]_2[TCNE]_2$ was carried out under an inert atmosphere. A solution of [Mepy]I (421 mg, 1.91 mmol) in 4 mL acetonitrile was slowly added to a rapidly stirring solution of TCNE (148 mg, 1.16 mmol) in 3 mL of acetonitrile. The solution volume was reduced to 3 mL by applying a vacuum, and then placed in a freezer at −30 °C. The resulting purple crystals were filtered off and then recrystallized twice from acetonitrile. IR (KBr/cm^{-1}) : $\nu_{C\equiv N}$ 2268 (w) (MeCN), 2243 (w) (MeCN), 2191 (s), 2174 (m), 2169 (m), 2163 (sh); ν_{CC} 1366 (s). UV/Vis (KBr/cm^{-1}) : 26,880, 18,520.

Crystal structure determination

X-Ray diffraction. A dataset was collected from a single crystal (0.35 × 0.40 × 0.40 mm) at 50(2) K using graphite monochromated Mo Kα radiation on a Bruker Smart 1000 fitted with a CCD detector and Oxford Cryosystems HeliX. Structure solution was carried out and refined by full matrix least squares using the SHELX suite.[10] All non-hydrogen atoms were refined with anisotropic displacement parameters. Hydrogen atoms were positioned geometrically with isotropic displacement parameters fixed to ride on the parent atom [aromatic C–H 0.94 Å, $U_{iso} = 1.2 \times U_{eq}$(C); methyl C–H 0.98 Å, $U_{iso} = 1.5 \times U_{eq}$(C)]. No disorder of the methyl group was apparent at 50 K. The crystallographic information is summarized in Table 1. The structure had also been determined at 150(1) K and the methyl groups of the cation were found to be disordered over two orientations with a 60.0° rotation between the two orientations in a 3 : 2 ratio.

Neutron diffraction. Neutron diffraction data were obtained at the intense pulsed neutron source (IPNS) at ANL using the time-of-flight Laue single crystal diffractometer (SCD).[11,12] At the IPNS, pulses of protons are accelerated into a heavy-element target 30 times a second to produce pulses of neutrons by the spallation process. Because of the pulsed nature of the source, neutron wavelengths are determined by time-of-flight based on the de Broglie equation $\lambda = ht/ml$, where h is Planck's constant, m is the neutron mass, and t is the time-of-flight for a flight path l, so that the entire thermal spectrum of neutrons can be used. With position-sensitive area detectors and a range of neutron wavelengths, a solid volume of reciprocal space is sampled with each stationary orientation of the sample and the detectors. The SCD has two ^{6}Li-glass scintillation position-sensitive area detectors, each with active areas of 15 × 15 cm and a spatial resolution of < 1.5 mm. One of the detectors is centered at a scattering angle of 75° and a crystal-to-detector distance of 23 cm, and the second detector is at 120° and 18 cm. Details of the data collection and analysis procedures have been published previously.[11,12]

A ~1 × 3.5 × 4 mm crystal was wrapped in aluminium foil, glued to an aluminium pin in a glove bag, and then was mounted on the cold stage of a closed-cycle helium refrigerator and cooled to 50 ± 1 K. For each setting of the diffractometer angles, data were stored in a 3D histogram form with coordinates x,y,t corresponding to horizontal and vertical detector positions and the time-of-flight, respectively. Data were analyzed using the ISAW software package[13] in addition to other local IPNS SCD programs. For intensity data collection, runs of 6 h per histogram were initiated, and covered a unique quadrant of reciprocal space (Laue symmetry $2/m$). Using this strategy, 17 histograms were completed during the 6 days available for the experiment.

Bragg reflections were integrated about their predicted location and were corrected for the Lorentz factor, the incident spectrum and the detector efficiency. The intensities were also corrected for absorption with wavelength-dependent linear absorption coefficients of [μ(cm^{-1}) = 1.047 + 0.575 λ] derived from cross sections for non-hydrogen[14] and hydrogen[15] atoms. Symmetry-related reflections were not averaged, since different extinction factors are applicable to reflections measured at different wavelengths. The GSAS software package was used for structural analysis.[16] The atomic positions of the X-ray diffraction structure were used as a starting point in the refinement, with the exception of the methyl group hydrogen atoms. These hydrogen atoms were confidently located in difference Fourier syntheses. The refinement was based on F^2 using 2528 reflections with a minimum d-spacing of 0.5 Å. Weights were assigned as $w(F_o^2) = 1/[(\sigma(F_o^2) + (0.002F_o^2)]^2$ where $\sigma^2(F_o^2)$ is the variance based on counting statistics. A Lorentzian Type-I extinction correction was applied. In the final refinement all atoms were refined with anisotropic displacement parameters. After final refinement the maximum peak of unmodeled scattering-density in the difference Fourier map was 0.21 cm × 10^{-12} Å^{-3}, which compares to approximately 4% of the peak maximum of a nitrogen atom in a Fourier map. The final least squares refinement was based upon 260 variables and converged to $R_w(F^2) = 0.155$ and $R(F^2) = 0.138$.

Table 1 X-Ray and neutron diffraction crystallographic data for $[Mepy]_2[TCNE]_2$ at 50 K

	Neutron	X-Ray
Empirical formula	$C_{12}H_8N_5$	$C_{12}H_8N_5$
Formula mass	222.23	222.23
Space group	$P2_1/n$	$P2_1/n$
a/Å	6.731(1)	6.7484(2)
b/Å	9.996(2)	10.0584(3)
c/Å	16.489(4)	16.5583(5)
β/°	95.235(19)	95.276(1)
V/Å^3	1104.887(416)	1119.18(6)
Z	4	4
ρ_{calc}/g cm^{-3}	1.337	1.319
μ/cm^{-1}	1.047 + 0.575 λ	0.086
T/K	50(1)	50(2)
λ/Å	0.4–10.0 [f]	0.71073 MoK_α
Reflections collected	3749	18183
Unique reflections		3365 (R_{int} = 0.0252)
R index[a] [$I > 2\sigma(I)$]		R_1 = 0.0368, wR_2 = 0.0920
No. of refins	2528 [$I > 3\sigma(I)$][b]	2830 [$I > 2\sigma I$]
R indices[a] (all data)	Rw 0.155,[c] R = 0.138[d]	$R1$ = 0.0460,[a] $wR2$ = 0.0974[a]
Goodness-of-fit[e] on F^2	1.544	1.042

[a] $R1 = \frac{\sum \left||F_o| - |F_c|\right|}{\sum |F_o|}$; $wR2 = \sqrt{\frac{\sum \left[w(F_o^2 - F_c^2)^2\right]}{\sum \left[w(F_o^2)^2\right]}}$ where $w^{-1} = [\sigma^2(F_o^2) + (aP)^2 + bP]$ and $P = \frac{(F_o^2 + 2F_c^2)}{3}$. [b] Data with $F_o^2/F_c^2 > 2$ were rejected. [c] $R_w(F^2) = \{\sum[w(F_o^2 - F_c^2)^2]/\sum[w(F_o^2)^2]\}^{1/2}$. [d] $R(F^2) = \Sigma|F_o^2 - F_c^2|/\Sigma|F_o^2|$. [e] GooF = $S = \sqrt{\frac{\sum \left[w(F_o^2 - F_c^2)^2\right]}{(M - N)}}$, M = number of reflections; N = number of parameters refined. [f] Neutron time-of-flight Laue.

Spectroscopic studies

Infrared spectra were taken using a Bruker Tensor 37 FTIR spectrophotometer with ±1 cm^{-1} resolution, and scanned in the range of 400 to 4000 cm^{-1}. UV/Visible spectroscopy was carried out on a Hewlett Packard 8452A Diode Array Spectrophotometer from 190 to 820 nm. Samples were prepared as KBr pressed pellets (~5% w/w) for both experiments.

Results and discussion

The reaction of [Mepy]I and TCNE leads to the formation of $[Mepy]_2[TCNE]_2$, eqn (1), and $[Mepy]I_3$. $[Mepy]_2[TCNE]_2$

Fig. 2 Large bronze-reflecting crystal of $[Mepy]_2[TCNE]_2$ grown from MeCN.

crystallizes prior to $[Mepy]I_3$, and was exclusively collected by careful observation during crystallization. The structure of $[Mepy]_2[TCNE]_2$ was initially determined *via* X-ray diffraction and subsequently studied by neutron diffraction given the availability of large (14 mm^3) single crystals (Fig. 2).

$$3\,[Mepy]^+ + 3\,I^- + 2\,TCNE \rightarrow [Mepy]I_3 + [Mepy]_2[TCNE]_2 \quad (1)$$

The structure consists of a centrosymmetric π-$[TCNE]_2^{2-}$ dimer, the asymmetric unit of which is depicted in Fig. 3. Close approach between the two $[TCNE]^-$ anions results in an eclipsed dimer with an intradimer separation of 2.806(1) Å at 50 K between olefinic carbon atoms. The central C2–C4 bond distance on each $[TCNE]^-$ moiety is 1.425(1) Å, and the cyano groups bend away from the center of the dimer to accommodate this interaction. Thus, C2 and C4 deviate by 0.15(1) Å from the plane containing C1, C3, C5, C6 at 50 K, and the CN's move away of the $[TCNE]^-$ plane by an average value of 6.9° at 50 K.[17] The key distances and angles are tabulated in Tables 2 and 3. The methyl group of the $[Mepy]^+$ cation displays rotational disorder over two

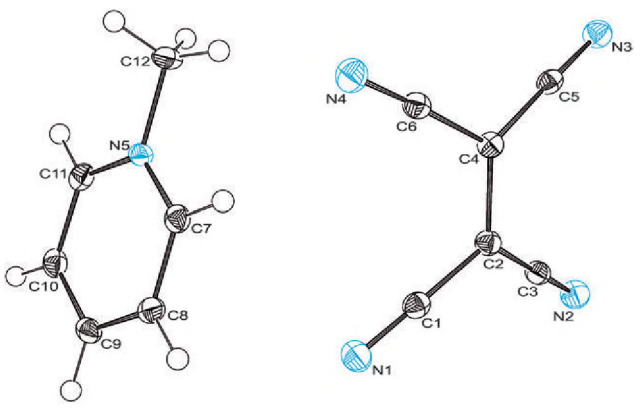

Fig. 3 Atom labeling and plot of the symmetry independent components of $[Mepy]_2[TCNE]_2$ with thermal ellipsoids of the non-hydrogen atoms depicted at the 50% probability level derived from the 50-K X-ray data.

Table 2 Key bond distances for $[Mepy]_2[TCNE]_2$ (Å)

Atoms	X-Ray, 50 K Distance	Neutron, 50 K Distance	Atoms	X-Ray, 50 K Distance	Neutron, 50 K Distance
N1–C1	1.155(1)	1.156(4)	C2–C3	1.422(1)	1.406(4)
N2–C3	1.155(1)	1.154(3)	C2–C4	1.425(1)	1.423(4)
N3–C5	1.156(1)	1.158(4)	C4–C5	1.420(1)	1.411(4)
N4–C6	1.154(1)	1.148(3)	C4–C6	1.423(1)	1.408(4)
N5–C7	1.347(1)	1.339(3)	C7–C8	1.380(1)	1.379(4)
N5–C11	1.349(1)	1.351(3)	C8–C9	1.388(1)	1.381(4)
N5–C12	1.479(1)	1.468(4)	C9–C10	1.388(1)	1.389(4)
C1–C2	1.422(1)	1.414(4)	C10–C11	1.378(1)	1.382(4)

Table 3 Key bond angles for $[Mepy]_2[TCNE]_2$ (°) at 50 K

Atoms	X-Ray, 50 K Angle	Neutron, 50 K Angle	Atoms	X-Ray, 50 K Angle	Neutron, 50 K Angle
C7–N5–C11	121.32(8)	121.2(2)	C2–C4–C6	119.71(8)	119.2(3)
C7–N5–C12	119.89(8)	119.8(2)	C5–C4–C6	120.88(8)	119.1(2)
C11–N5–C12	118.78(8)	119.0(2)	N3–C5–C4	178.44(9)	179.3(3)
N1–C1–C2	178.06(10)	178.0(3)	N4–C6–C4	177.07(10)	177.2(3)
C1–C2–C3	117.13(8)	117.1(3)	N5–C7–C8	120.27(8)	120.5(3)
C1–C2–C4	120.31(8)	120.6(2)	C7–C8–C9	119.19(9)	118.8(3)
C3–C2–C4	120.93(8)	121.1(3)	C8–C9–C10	119.70(9)	120.7(3)
N2–C3–C2	178.82(10)	178.1(3)	C9–C10–C11	119.00(9)	117.8(3)
C2–C4–C5	120.88(8)	120.3(2)	N5–C11–C10	120.52(8)	120.9(3)

positions at 150 K, but this disorder is frozen out at 50 K. The solid-state structure consists of dimerized zigzag chains of $[TCNE]_2^{2-}$ with intra- and interdimer separations of 2.806(1) (C4–C2a; a = $-x$, $1-y$, $-z$) and 4.061(2) Å (C4–C4b; b = $1-x$, $1-y$, $-z$), respectively (Fig. 4). Despite the short intradimer C···C separations between pairs of $[TCNE]^-$ anions the species did not undergo a solid state cycloaddition reaction upon irradiation with broad band UV light; as no change in the crystal structure or diffraction quality was noted after 18 h irradiation at 180 K.

The 50-K neutron diffraction shows the same basic structural features as shown in Fig. 3, with the intradimer separation being 2.801(4) Å, and a central TCNE C–C bond distance of 1.423(4) Å. The CN's groups lie out of the $[TCNE]^-$ plane by an average value of 6.7°.[17] The key distances and angles are tabulated in

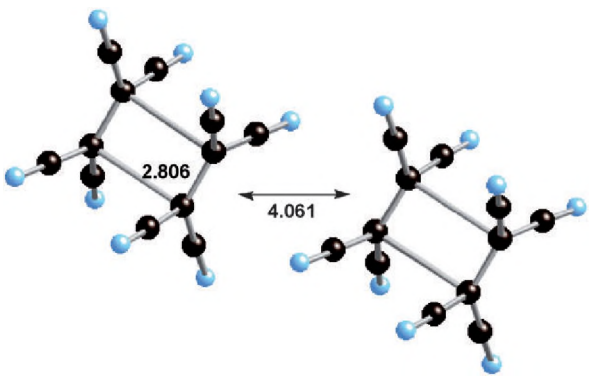

Fig. 4 Intra- and interdimer $[TCNE]_2^{2-}$ interactions in $[Mepy]_2[TCNE]_2$ distances at 50 K.

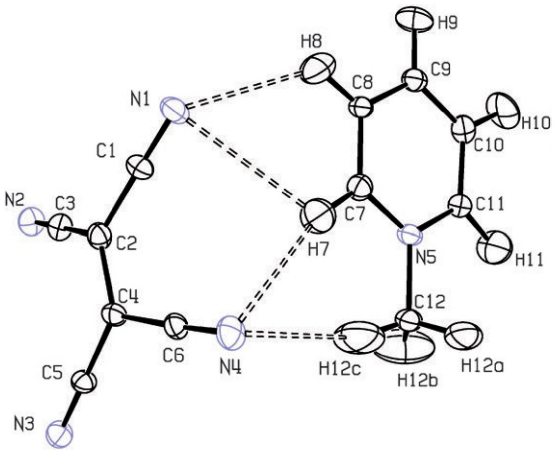

Fig. 5 Atom labeling and thermal ellipsoid (50%) plot of asymmetric unit of $[Mepy]_2[TCNE]_2$ determined at 50 K *via* neutron diffraction. Dashed lines indicate four of the seven C–H···N contacts that are at, or below, the sum of the van der Waals radii for hydrogen and nitrogen (2.75 Å).

Tables 2 and 3; intradimer distances and torsion angles are listed in Table S1.† Neutron diffraction data were used to accurately determine the location of the hydrogen atoms and close C–H···N interactions were examined between the cation and anion(s), which may stabilize a long intradimer C–C bond. Fig. 5 presents the molecular structure of the asymmetric unit. Close nonbonding contacts may be identified by examining distances shorter than those found for the sum of the van der Waals radii of the atoms in question. For hydrogen (1.20 Å) and nitrogen (1.55 Å) the sum of the radii is equal to 2.75 Å,[18] and thus all 13 H···N distances less than 3 Å were examined. The lists of these distances and associated angles are found in Tables S2 and S3.† Seven of these distances fall at or below the sum of the van der Waals radii, within statistical error. There has been some debate in the literature over whether these short contacts constitute traditional hydrogen bonds.[19,20,21] While these H···N contacts are short and may fall into the range appropriate for classical hydrogen bonding, the angles in Table S3† indicate a distinct "lack of directional behavior" or near linearity that may be necessary to classify them definitively as hydrogen bonds.[19,20] For example, the shortest contacts of H9–N2 (2.45 Å) and H8–N1 (2.52 Å) have C–H···N angles of 128.4 and 125.3°, respectively. Conversely, the two potential interactions with the larger C–H···N angles (165.0 and 158.6°) have distances that are at or above the sum of the van der Waals contact (H7–N4 = 2.77 Å and H12c–N4 = 2.98 Å), leaving no clear correlation between H···N distance and directionality of the contact. However, the short H···N contacts and the wide range of angles may direct the crystal packing forces, stabilizing the close π–π contact between the TCNE anions. As many of these H···N contacts are clearly less than the sum of the van der Waals radii but non-directional it may then be more appropriate to term these weak interactions as "hydrogen bridges".[21]

Irrespective of the hydrogen bonding, $[TCNE]_2^{2-}$ is a π dimer that is best described by a two-electron four-centered bond between the $[TCNE]^-$ monomer moieties.[3] Dimerization of $[TCNE]^-$ leads to overlap of the b_{2g} singly occupied molecular orbital (SOMO) on each moiety to form bonding and antibonding orbitals of b_{2u} and b_{1g} symmetry (Fig. 1), respectively, with an $^1A_{1g}$ ($b_{2u}^2b_{1g}^0$) ground state electronic structure for the dimer.

The intradimer C–C bond distance of 2.806(1) Å is comparable to those previously reported that range from 2.83 to 3.09 Å.[3] Another manifestation of the intradimer C–C bonding is the change in hybridization of the central carbons, which results in C2 and C4 deviating by 0.15(1) Å from a plane defined by C1, C3, C5 and C6. This is additionally noted by the *trans*–NC–C–C–CN angle increasing from 0° for planar $[TCNE]^-$ to an average value of 6.7°[17] for $[Mepy]_2[TCNE]_2$. This is in accord with those reported previously that range from 3.6 to 6.5°.[3]

Intradimer $[TCNE]_2^{2-}$ bond formation also leads to a change in the IR spectrum, which differs with respect to its constituent fragments, *i.e.* two $[TCNE]^{\bullet-}$ where the ν_{CN} IR absorptions occur at 2183 and 2144 cm^{-1},[3,22] while the ν_{CC} is IR inactive and not observed. In contrast, as previously reported π-$[TCNE]_2^{2-}$ exhibits three $\nu_{C\equiv N}$ vibrations at 2191 ± 2 (m), 2172 ± 2 (s), and 2161 ± 2 (s) cm^{-1} and the ν_{CC} at 1360 (s) cm^{-1}.[3,5] For $[Mepy]_2[TCNE]_2$ these IR bands occur at 2191 (m), 2174 (m), 2169 (m), 2163 (m) ($\nu_{C\equiv N}$), and 1366 (s) cm^{-1} (ν_{CC}) for $[Mepy]_2[TCNE]_2$ are consistent with the formation of a $[TCNE]_2^{2-}$ dimer. The ~1360-cm^{-1} absorption is the antisymmetric combination of the intrafragment C–C stretches of each central C–C bond, which becomes allowed and gains intensity due to electron-vibrational coupling.[23]

The electronic absorption spectrum of $[TCNE]^{\bullet-}$ has an absorption at 23 375 cm^{-1} (428 nm; 2.89 eV) in solution, which has 17 vibrational overtones.[22] This $^2B_{2u} \rightarrow {}^2B_{3g}$ transition broadens in the solid state. In $[Mepy]_2[TCNE]_2$, $[TCNE]_2^{2-}$ also exhibits a broad absorption at 26 880 cm^{-1} (372 nm; 3.33 eV) as well as an additional absorption at 18 520 cm^{-1} (540 nm; 2.30 eV) (Fig. 6). The latter absorption is assigned to the $b_{2u}^2b_{1g}^0$ ($^1A_{1g}$) → $b_{2u}^1b_{1g}^1$ ($^1B_{1u}$) transition and gives these dimeric compounds the observed dark blue–purple color. This value is higher in energy than the 15 300 cm^{-1} (654 nm, 1.90 eV) reported for $Tl_2[TCNE]_2$, $[(Me_2N)_2CC(NMe_2)_2][TCNE]_2$, and $[Cr^I(C_6H_6)]_2[TCNE]_2$.[3,5]

Intradimer bond formation also affects the magnetic properties. When doublet $S = 1/2$ $[TCNE]^{\bullet-}$ fragments approach each

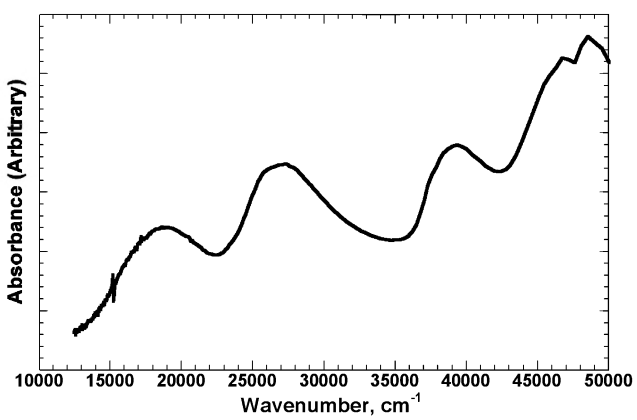

Fig. 6 Solid-state UV-Vis spectra $[TCNE]_2^{2-}$ in $[Mepy]_2[TCNE]_2$.

other to form the π-$[TCNE]_2^{2-}$ dimer, Fig. 4, the spins interact to form an $S = 0$ singlet ground state and an $S = 1$ triplet excited state (or *vice versa*). Strong antiferromagnetic coupling between the spins leads to the singlet ground state.[3] However, upon warming thermal population of the triplet excited state may be achieved, as has been frequently reported.[24] Similarly for related $[TCNE]_2^{2-}$ dimers,[3] diamagnetic-like behavior is observed for $[Mepy]_2[TCNE]_2$ due to only the singlet state being populated below room temperature.

Conclusion

The neutron data provide accurate structural parameters for the $[TCNE]_2^{2-}$ dimer, and the detailed analysis of the cation hydrogen···$[TCNE]_2^{2-}$ interactions, while best described as "hydrogen bridges," do not stabilize the $[TCNE]_2^{2-}$ dimer. $[Mepy]_2[TCNE]_2$ possesses $[TCNE]_2^{2-}$ dimers with an intradimer C2–C4 bond distance from X-ray diffraction of 2.806(1) Å at 50 K [2.822(1) Å at 150 K)] The nitriles bend away from the centre of the dimer, with C2 and C4 deviating by 0.15(1) Å from a plane containing C1, C3, C5 and C6, and the CN's groups move away of the $[TCNE]^-$ plane by an average value of 6.8°. This bonding is best described as a two-electron four-centered bond between the four central carbon atoms within the pair of $[TCNE]^-$ moieties that are related by an inversion centre. As a consequence, the $[TCNE]_2^{2-}$ dimers exhibit $\nu_{C\equiv N}$ at 2191, 2174, 2169 (shoulder), 2163 and ν_{CC} at 1366 cm^{-1} in the IR, and electronic $^1A_{1g} \rightarrow {}^1B_1$ absorption bands at 26 880 and 18 520 cm^{-1} in the UV-vis spectrum.

Acknowledgements

The authors gratefully acknowledge the discussions with Juan J. Novoa (University of Barcelona), and sample preparation by Michelle L. Taliaferro and Joshua Bell, and the support from the NSF (Grant No. CHE0110685), the DOE (Grant No. DE FG 03-93ER45504). Work at Argonne was supported by the US Department of Energy, BES-Materials Science, under Contract DE-AC02-06CH11357. J.A.K.H. and H.A.S. are grateful to the EPSRC for funding (EP/E048994/1) and Durham University for facilities.

References

1 G. Kaupp and J. Boy, *Angew. Chem., Int. Ed.*, 1997, **36**, 48.
2 F. Toda, *Eur. J. Org. Chem.*, 2000, 1377.
3 J. J. Novoa, P. Lafuente, R. E. Del Sesto and J. S. Miller, *Angew. Chem., Int. Ed.*, 2001, **40**, 2540.
4 J. Llop, C. Viñas, C. J. M. Oliva, F. Teixidor, M. A. Flores, R. Kivekas and R. Sillanpää, *J. Organomet. Chem.*, 2002, **657**, 232; F. Teixidor and C. Viñas, *Sci. Synth.*, 2005, **6**, 1235; D. A. Brown, W. Clegg, H. M. Colquhoun, J. A. Daniels, I. R. Stephenson and K. A. Wade, *J. Chem. Soc., Chem. Commun.*, 1987, 889; J. Llop, C. Viñas, F. Teixidor, L. Victori, R. Kivekäs and R. Sillanpää, *Inorg. Chem.*, 2002, **41**, 3347.
5 R. E. Del Sesto, J. S. Miller, J. J. Novoa and P. Lafuente, *Chem.–Eur. J.*, 2002, **8**, 4894.
6 J. Jakowski and J. Simons, *J. Am. Chem. Soc.*, 2003, **124**, 16089; J. K. Kochi, R. Rathore and P. Le Magneres, *J. Org. Chem.*, 2000, **65**, 6826; Y. Jung and M. Head-Gordon, *Phys. Chem. Chem. Phys.*, 2004, **6**, 2008.
7 J. S. Miller and J. J. Novoa, *J. Acc. Chem. Res.*, 2007, **40**, 189.
8 M. T. Johnson, C. F. Campana, B. M. Foxman, W. Desmarais, M. J. Vela and J. S. Miller, *Eur. J. Chem.*, 2000, **6**, 1805.
9 J. R. Fox, B. M. Foxman, D. Guerrer, J. S. Miller and A. H. Reis, Jr., *J. Mater. Chem.*, 1996, **6**, 1627.
10 G. M. Sheldrick, *Acta Crystallogr., Sect. A*, 1990, **46**, 467.
11 A. J. Schultz, K. Srinivasan, R. G. Teller, J. M. Williams and C. M Lukehart, *J. Am. Chem. Soc.*, 1984, **106**, 999.
12 A. J. Schultz, P. M. De Lurgio, J. P. Hammonds, D. J. Mikkelson, R. L. Mikkelson, M. E. Miller, I. Naday, P. F. Peterson, R. R. Porter and T. G. Worlton, *Physica B*, 2006, **385–386**, 1059.
13 A. Chatterjee, D. Mikkelson, R. Mikkelson, J. Hammonds and T. Worlton, *Appl. Phys. A: Mater. Sci. Process.*, 2002, **74**, 194.
14 V. F. Sears, in *Methods of Experimental Physics, Vol. 23, Neutron Scattering, Part A*, ed. K. Sköld and D. L. Price, Academic Press: Orlando, FL, 1986, pp 521.
15 J. A. K. Howard, O. Johnson, A. J. Schultz and A. M. Stringer, *J. Appl. Crystallogr.*, 1987, **20**, 120.
16 A. C. Larson, and R. B. Von Dreele, *General Structure Analysis System-GSAS*, Los Alamos National Laboratory, 2000.
17 Calculated from one-half of the average *trans*–NC–C–C–CN dihedral angles using CrystalMaker8.
18 A. Bondi, *J. Phys. Chem.*, 1964, **68**, 441.
19 F. A. Cotton, L. M. Daniels, G. T. Jordan and C. A. Murillo, *Chem. Commun.*, 1997, 1673.
20 T. Steiner and G. R. Desiraju, *Chem. Commun.*, 1998, 891.
21 G. R. Desiraju, *Acc. Chem. Res.*, 2002, **35**, 565.
22 D. L. Jeanmarie, M. R Suchanski and R. P. Van Duyne, *J. Am. Chem. Soc.*, 1975, **97**, 1699; D. A. Dixon and J. S. Miller, *J. Am. Chem. Soc.*, 1987, **109**, 3656.
23 Similar results were noted for $(TCNQ)_2^{2-}$: M. J. Rice, N. O. Lipari and S. Strassler, *Phys. Rev. Lett.*, 1977, **39**, 1359.
24 *e.g.*, B. Bleaney and K. D. Bowers, *Proc. R. Soc. London, Ser. A*, 1952, **214**, 451; K. M. Chi, J. C. Calabrese and J. S. Miller, *Mol. Cryst., Liq. Cryst.*, 1989, **176**, 173.